

Conformational change of *N*-benzylideneanilines in crystals

Jun Harada, Mayuko Harakawa
and Keiichiro Ogawa*

Department of Chemistry, Graduate School of
Arts and Sciences, The University of Tokyo,
Komaba, Meguro-ku, Tokyo 153-8902, Japan

Correspondence e-mail:
ogawa@ramie.c.u-tokyo.ac.jp

Received 7 April 2004
Accepted 7 July 2004

The crystal structures of *N*-(4-nitrobenzylidene)aniline (1), *N*-(4-chlorobenzylidene)-4-methylaniline (2) and *N*-(4-methylbenzylidene)-4-methylaniline (3) were determined by X-ray diffraction analyses at various temperatures. A dynamic disorder was observed in the crystal structures of all compounds. The dynamic disorder is accounted for in terms of a conformational change involving a pedal motion in the crystals.

1. Introduction

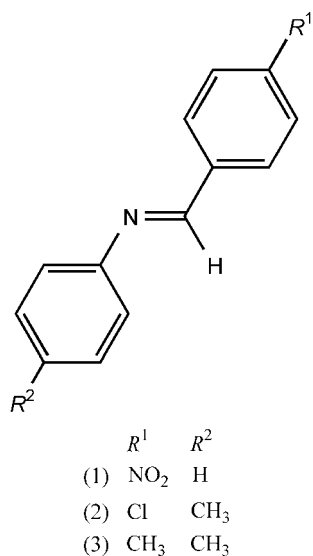
Solid-state conformational changes have been studied in a wide range of fields in chemistry (Gavezzotti & Simonetta, 1982, 1987; Harris & Aliev, 1995; Bürgi, 2002). Among the several methods that have been applied to the subject, X-ray diffraction analysis is one of the most powerful. When conformational changes take place in crystals, each molecule adopts one of several possible, alternative conformations. X-ray diffraction studies give access to the populations of each conformer by analysis of diffraction data with a disorder model. The occurrence of conformational changes in crystals can be detected on the basis of temperature-dependent populations of the conformers. Thus, variable-temperature X-ray diffraction measurement and analysis of the disorder provide not only static molecular structures, but also substantial information on the dynamic aspects of molecules in the crystals.

We have studied the conformational changes of (*E*)-stilbenes and azobenzenes in crystals using disorder analysis (Harada *et al.*, 1997; Harada & Ogawa, 2001, 2004). In the disordered crystals of these compounds the molecules adopt two orientations related by an approximate twofold rotation about the longest axis of the molecules (Fig. 1).

Variable-temperature X-ray diffraction analyses showed that the populations depend on the temperature, which behavior is indicative of a conformational interconversion in the crystal. The conformational change was inferred to take place through a pedal motion: a pair of benzene rings moving like the pedals of a bicycle (Fig. 2). Solid-state NMR spectroscopy (Ueda *et al.*, 1988; McGeorge *et al.*, 1998), measurements of heat capacity (Saito *et al.*, 1995, 2000, 2004) and molecular mechanics calculations (Galli *et al.*, 1999) have substantiated the occurrence of the pedal motion. The same motion was reported to be a key process of the photochromism of salicylideneanilines and the photodimerization of *trans*-cinnamides in the crystalline state (Harada *et al.*, 1999; Ito *et al.*, 2000; Ohba *et al.*, 2001).

In this study we investigated the solid-state conformational change of some derivatives of *N*-benzylideneaniline, which is isoelectronic with (*E*)-stilbene and azobenzene. Although the

crystal structures of some *N*-benzylideneanilines are known to show a disorder similar to that observed for (*E*)-stilbenes and azobenzenes (Bernstein *et al.*, 1976; Bar & Bernstein, 1983), the dynamic properties of the disorder have yet to be studied. In the preceding paper we described the results of the variable-temperature X-ray diffraction analyses of some *N*-benzylideneanilines and showed that a torsional vibration about the C–Ph and N–Ph bonds, which is similar to the pedal motion, takes place in the crystals (Harada *et al.*, 2004). In this paper we report on the variable-temperature X-ray diffraction analyses of some additional disordered *N*-benzylideneanilines: *N*-(4-nitrobenzylidene)aniline (1), *N*-(4-chlorobenzylidene)-4-methylaniline (2) and *N*-(4-methylbenzylidene)-4-methylaniline (3). Disorder analyses of the crystal structures revealed that disorder in the crystals of these *N*-benzylideneanilines is dynamic and that conformational changes through pedal motion take place. Detailed analysis of the temperature dependence of the crystal structure of (3) showed that conformational changes may be frozen in, so that nonequilibrium states are found at low temperature.



2. Experimental

All compounds were obtained by the dehydration condensation between corresponding benzaldehydes and anilines. Crystals of (1) and (2) were obtained by recrystallization from methanol. Crystals of (3) were obtained from ethanol. Melting points were determined on a micro-hot-stage apparatus and are uncorrected.

All diffraction measurements were carried out using a Bruker SMART 1000 CCD area-detector system with graphite-monochromated Mo $K\alpha$ radiation ($\lambda = 0.71073 \text{ \AA}$). Approximately 2500 frames of data were collected per data set with a scan width of 0.3° in ω and 5 or 10 s exposure times. A semi-empirical absorption correction was applied to the data using the *SADABS* program (Sheldrick, 2002). The temperature of the crystals was controlled using a Cryostream (Oxford

Cryosystems) open-flow gas cryostat (Cosier & Glazer, 1986), except for the measurements at room temperature. The temperature in the nozzle was held constant within $\pm 0.2 \text{ K}$ during the measurement. The crystals were cooled or warmed at a rate of 1 K min^{-1} , unless otherwise mentioned. The crystal and experimental data are summarized in Table 1.

Three sets of diffraction data (at room temperature, 200 K and 90 K) were collected for (1) and (2). The temperature dependence of the crystal structure of (3) was investigated in more detail. A total of 10 sets of diffraction data were collected at various temperatures using the same crystal, seven of which are discussed in this paper. Temperature changes and diffraction measurements were carried out according to the following procedures. Diffraction measurements were carried out at 300, 250, 200, 150 and 90 K in this order. Before each measurement the crystal was warmed to room temperature

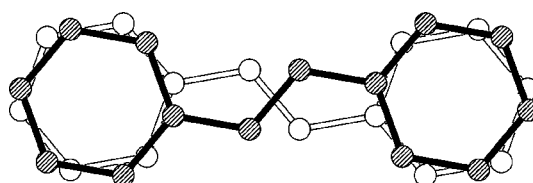


Figure 1
Disorder for stilbenes and azobenzenes.

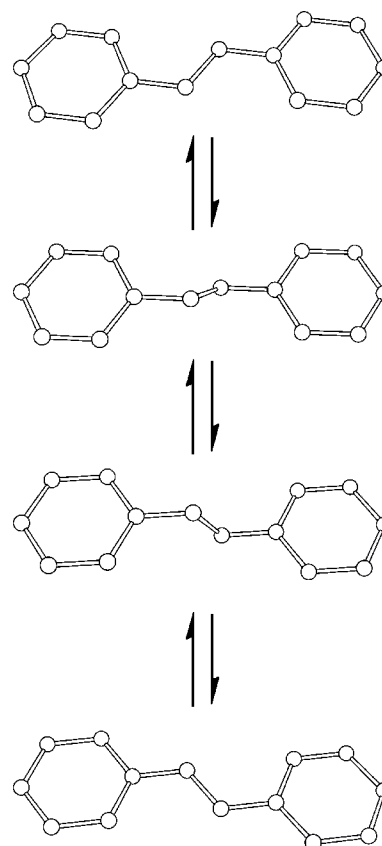


Figure 2
Pedal motion of stilbenes and azobenzenes.

Table 1
Experimental details.

	(1) at RT	(1) at 200 K	(1) at 90 K	(2) at RT
Crystal data				
Chemical formula	C ₁₃ H ₁₀ N ₂ O ₂	C ₁₃ H ₁₀ N ₂ O ₂	C ₁₃ H ₁₀ N ₂ O ₂	C ₁₄ H ₁₂ ClN
<i>M_r</i>	226.23	226.23	226.23	229.70
Cell setting, space group	Monoclinic, <i>P</i> ₂ ₁ / <i>n</i>	Monoclinic, <i>P</i> ₂ ₁ / <i>n</i>	Monoclinic, <i>P</i> ₂ ₁ / <i>n</i>	Monoclinic, <i>P</i> ₂ ₁ / <i>a</i>
<i>a</i> , <i>b</i> , <i>c</i> (Å)	14.6363 (11), 10.8175 (8), 14.7228 (11)	14.4053 (11), 10.7367 (8), 14.7627 (12)	14.2105 (12), 10.6596 (9), 14.8045 (12)	5.9663 (5), 7.3989 (7), 13.7221 (12)
β (°)	101.943 (1)	101.617 (2)	101.228 (2)	99.120 (2)
<i>V</i> (Å ³)	2280.6 (3)	2236.5 (3)	2199.6 (3)	598.09 (9)
<i>Z</i>	8	8	8	2
<i>D_x</i> (Mg m ⁻³)	1.318	1.344	1.366	1.275
Radiation type	Mo <i>K</i> α	Mo <i>K</i> α	Mo <i>K</i> α	Mo <i>K</i> α
No. of reflections for cell parameters	7219	10 646	13 353	3013
θ range (°)	2.2–28.5	2.4–29.5	2.2–30.0	2.8–30.0
μ (mm ⁻¹)	0.09	0.09	0.10	0.29
Temperature (K)	300	200	90	300
Crystal form, colour	Block, yellow	Block, yellow	Block, yellow	Block, colourless
Crystal size (mm)	0.46 × 0.40 × 0.28	0.46 × 0.40 × 0.28	0.46 × 0.40 × 0.28	0.48 × 0.34 × 0.18
Data collection				
Diffractometer	Bruker SMART 1000CCD diffractometer	Bruker SMART 1000CCD diffractometer	Bruker SMART 1000CCD diffractometer	Bruker SMART 1000CCD diffractometer
Data collection method	ω scan	ω scan	ω scan	ω scan
Absorption correction	Multi-scan (based on symmetry-related measurements)	Multi-scan (based on symmetry-related measurements)	Multi-scan (based on symmetry-related measurements)	Multi-scan (based on symmetry-related measurements)
<i>T_{min}</i>	0.959	0.959	0.958	0.874
<i>T_{max}</i>	0.975	0.974	0.974	0.950
No. of measured, independent and observed reflections	34 291, 6663, 3616	33 619, 6529, 4886	33 043, 6400, 5521	8950, 1760, 1271
Criterion for observed reflections	<i>I</i> > 2σ(<i>I</i>)	<i>I</i> > 2σ(<i>I</i>)	<i>I</i> > 2σ(<i>I</i>)	<i>I</i> > 2σ(<i>I</i>)
<i>R_{int}</i>	0.041	0.024	0.023	0.019
θ _{max} (°)	30.1	30.0	30.0	30.0
Range of <i>h</i> , <i>k</i> , <i>l</i>	−20 ⇒ <i>h</i> ⇒ 20 −15 ⇒ <i>k</i> ⇒ 15 −20 ⇒ <i>l</i> ⇒ 20	−20 ⇒ <i>h</i> ⇒ 20 −15 ⇒ <i>k</i> ⇒ 15 −20 ⇒ <i>l</i> ⇒ 20	−20 ⇒ <i>h</i> ⇒ 19 −15 ⇒ <i>k</i> ⇒ 15 −20 ⇒ <i>l</i> ⇒ 20	−8 ⇒ <i>h</i> ⇒ 8 −10 ⇒ <i>k</i> ⇒ 10 −19 ⇒ <i>l</i> ⇒ 19
Refinement				
Refinement on	<i>F</i> ²	<i>F</i> ²	<i>F</i> ²	<i>F</i> ²
<i>R</i> [<i>F</i> ² > 2σ(<i>F</i> ²)], <i>wR</i> (<i>F</i> ²), <i>S</i>	0.065, 0.174, 1.03	0.047, 0.131, 1.02	0.039, 0.112, 1.02	0.060, 0.195, 1.08
No. of reflections	6663	6529	6400	1760
No. of parameters	399	387	387	72
H-atom treatment	Mixture of independent and constrained refinement	Refined independently	Refined independently	Constrained to parent site
Weighting scheme	$w = 1/[\sigma^2(F_o^2) + (0.0436P)^2 + 0.878P]$, where $P = (F_o^2 + 2F_c^2)/3$	$w = 1/[\sigma^2(F_o^2) + (0.0542P)^2 + 0.6974P]$, where $P = (F_o^2 + 2F_c^2)/3$	$w = 1/[\sigma^2(F_o^2) + (0.0629P)^2 + 0.6739P]$, where $P = (F_o^2 + 2F_c^2)/3$	$w = 1/[\sigma^2(F_o^2) + (0.0841P)^2 + 0.1347P]$, where $P = (F_o^2 + 2F_c^2)/3$
(Δ/σ) _{max}	<0.0001	0.001	0.001	<0.0001
Δρ _{max} , Δρ _{min} (e Å ⁻³)	0.18, −0.29	0.27, −0.25	0.42, −0.19	0.24, −0.36
Extinction method	None	None	None	<i>SHELXL</i>
Extinction coefficient	–	–	–	0.101 (16)
	(2) at 200 K	(2) at 90 K	(3) at 300 K	(3) at 250 K
Crystal data				
Chemical formula	C ₁₄ H ₁₂ ClN	C ₁₄ H ₁₂ ClN	C ₁₅ H ₁₅ N	C ₁₅ H ₁₅ N
<i>M_r</i>	229.70	229.70	209.28	209.28
Cell setting, space group	Monoclinic, <i>P</i> ₂ ₁ / <i>a</i>	Monoclinic, <i>P</i> ₂ ₁ / <i>a</i>	Monoclinic, <i>P</i> ₂ ₁ / <i>c</i>	Monoclinic, <i>P</i> ₂ ₁ / <i>c</i>
<i>a</i> , <i>b</i> , <i>c</i> (Å)	5.9174 (5), 7.2879 (6), 13.70490 (11)	5.8827 (6), 7.1953 (7), 13.6919 (14)	9.8766 (7), 4.8839 (4), 12.0187 (9)	9.8649 (6), 4.8663 (3), 11.9484 (8)
β (°)	99.233 (2)	99.385 (2)	90.499 (1)	90.518 (1)
<i>V</i> (Å ³)	583.37 (7)	571.79 (10)	579.72 (8)	573.57 (6)
<i>Z</i>	2	2	2	2
<i>D_x</i> (Mg m ⁻³)	1.308	1.334	1.199	1.212
Radiation type	Mo <i>K</i> α	Mo <i>K</i> α	Mo <i>K</i> α	Mo <i>K</i> α
No. of reflections for cell parameters	5419	5419	2827	3145
θ range (°)	2.8–30.0	2.8–30.0	3.4–29.9	3.4–30.0

Table 1 (continued)

	(2) at 200 K	(2) at 90 K	(3) at 300 K	(3) at 250 K
μ (mm ⁻¹)	0.30	0.30	0.07	0.07
Temperature (K)	200	90	300	250
Crystal form, colour	Block, colourless	Block, colourless	Plate, colourless	Plate, colourless
Crystal size (mm)	0.48 × 0.34 × 0.18	0.48 × 0.34 × 0.18	0.40 × 0.30 × 0.08	0.40 × 0.30 × 0.08
Data collection				
Diffractometer	Bruker SMART 1000CCD diffractometer	Bruker SMART 1000CCD diffractometer	Bruker SMART 1000CCD diffractometer	Bruker SMART 1000CCD diffractometer
Data collection method	ω scan	ω scan	ω scan	ω scan
Absorption correction	Multi-scan (based on symmetry-related measurements)	Multi-scan (based on symmetry-related measurements)	Multi-scan (based on symmetry-related measurements)	Multi-scan (based on symmetry-related measurements)
T_{\min}	0.871	0.868	0.973	0.972
T_{\max}	0.949	0.948	0.995	0.994
No. of measured, independent and observed reflections	8648, 1707, 1454	8393, 1668, 1536	8496, 1689, 1330	8404, 1677, 1406
Criterion for observed reflections	$I > 2\sigma(I)$	$I > 2\sigma(I)$	$I > 2\sigma(I)$	$I > 2\sigma(I)$
R_{int}	0.016	0.017	0.022	0.019
θ_{max} (°)	30.0	30.0	30.0	30.0
Range of h, k, l	-8 ⇒ h ⇒ 8 -10 ⇒ k ⇒ 10 -19 ⇒ l ⇒ 19	-8 ⇒ h ⇒ 8 -10 ⇒ k ⇒ 10 -19 ⇒ l ⇒ 19	-13 ⇒ h ⇒ 13 -6 ⇒ k ⇒ 6 -16 ⇒ l ⇒ 16	-13 ⇒ h ⇒ 13 -6 ⇒ k ⇒ 6 -16 ⇒ l ⇒ 16
Refinement				
Refinement on	F^2	F^2	F^2	F^2
$R[F^2 > 2\sigma(F^2)], wR(F^2), S$	0.053, 0.148, 1.12	0.059, 0.141, 0.60	0.052, 0.149, 1.05	0.048, 0.135, 1.08
No. of reflections	1707	1668	1689	1677
No. of parameters	72	72	89	89
H-atom treatment	Constrained to parent site	Constrained to parent site	Constrained to parent site	Constrained to parent site
Weighting scheme	$w = 1/[\sigma^2(F_o^2) + (0.0574P)^2 + 0.1885P]$, where $P = (F_o^2 + 2F_c^2)/3$	$w = 1/[\sigma^2(F_o^2) + (0.0866P)^2 + 1.6982P]$, where $P = (F_o^2 + 2F_c^2)/3$	$w = 1/[\sigma^2(F_o^2) + (0.061P)^2 + 0.122P]$, where $P = (F_o^2 + 2F_c^2)/3$	$w = 1/[\sigma^2(F_o^2) + (0.0552P)^2 + 0.1239P]$, where $P = (F_o^2 + 2F_c^2)/3$
$(\Delta/\sigma)_{\text{max}}$	<0.0001	<0.0001	<0.0001	<0.0001
$\Delta\rho_{\text{max}}, \Delta\rho_{\text{min}}$ (e Å ⁻³)	0.29, -0.37	0.68, -0.65	0.23, -0.20	0.22, -0.20
Extinction method	SHELXL	SHELXL	SHELXL	SHELXL
Extinction coefficient	0.083 (10)	0.106 (10)	0.206 (18)	0.126 (13)
	(3) at 200 K	(3) at 150 K	(3) at 90 K	
Crystal data				
Chemical formula	C ₁₅ H ₁₅ N	C ₁₅ H ₁₅ N	C ₁₅ H ₁₅ N	
M_r	209.28	209.28	209.28	
Cell setting, space group	Monoclinic, $P2_1/c$	Monoclinic, $P2_1/c$	Monoclinic, $P2_1/c$	
a, b, c (Å)	9.8565 (6), 4.8494 (3), 11.8748 (7)	9.8477 (6), 4.8327 (3), 11.7991 (7)	9.8184 (6), 4.8159 (3), 11.7536 (7)	
β (°)	90.561 (1)	90.631 (1)	90.689 (1)	
V (Å ³)	567.57 (6)	561.50 (6)	555.72 (6)	
Z	2	2	2	
D_x (Mg m ⁻³)	1.225	1.238	1.251	
Radiation type	Mo $K\alpha$	Mo $K\alpha$	Mo $K\alpha$	
No. of reflections for cell parameters	3629	4040	4495	
θ range (°)	3.4–30.0	3.5–29.9	3.5–29.9	
μ (mm ⁻¹)	0.07	0.07	0.07	
Temperature (K)	200	150	90	
Crystal form, colour	Plate, colourless	Plate, colourless	Plate, colourless	
Crystal size (mm)	0.40 × 0.30 × 0.08	0.40 × 0.30 × 0.08	0.40 × 0.30 × 0.08	
Data collection				
Diffractometer	Bruker SMART 1000CCD diffractometer	Bruker SMART 1000CCD diffractometer	Bruker SMART 1000CCD diffractometer	
Data collection method	ω scan	ω scan	ω scan	
Absorption correction	Multi-scan (based on symmetry-related measurements)	Multi-scan (based on symmetry-related measurements)	Multi-scan (based on symmetry-related measurements)	
T_{\min}	0.972	0.972	0.972	
T_{\max}	0.994	0.994	0.994	

Table 1 (continued)

	(3) at 200 K	(3) at 150 K	(3) at 90 K
No. of measured, independent and observed reflections	8329, 1661, 1428	8213, 1641, 1453	8100, 1624, 1473
Criterion for observed reflections	$I > 2\sigma(I)$	$I > 2\sigma(I)$	$I > 2\sigma(I)$
R_{int}	0.017	0.015	0.013
θ_{max} (°)	30.0	30.0	30.0
Range of h, k, l	$-13 \Rightarrow h \Rightarrow 13$ $-6 \Rightarrow k \Rightarrow 6$ $-16 \Rightarrow l \Rightarrow 16$	$-13 \Rightarrow h \Rightarrow 13$ $-6 \Rightarrow k \Rightarrow 6$ $-16 \Rightarrow l \Rightarrow 16$	$-13 \Rightarrow h \Rightarrow 13$ $-6 \Rightarrow k \Rightarrow 6$ $-16 \Rightarrow l \Rightarrow 16$
Refinement			
Refinement on	F^2	F^2	F^2
$R[F^2 > 2\sigma(F^2)]$, $wR(F^2)$, S	0.045, 0.134, 1.08	0.043, 0.126, 1.06	0.041, 0.121, 1.07
No. of reflections	1661	1641	1624
No. of parameters	89	89	89
H-atom treatment	Constrained to parent site	Constrained to parent site	Constrained to parent site
Weighting scheme	$w = 1/[\sigma^2(F_o^2) + (0.0651P)^2 + 0.1155P]$, where $P = (F_o^2 + 2F_c^2)/3$	$w = 1/[\sigma^2(F_o^2) + (0.0652P)^2 + 0.132P]$, where $P = (F_o^2 + 2F_c^2)/3$	$w = 1/[\sigma^2(F_o^2) + (0.0687P)^2 + 0.1224P]$, where $P = (F_o^2 + 2F_c^2)/3$
$(\Delta/\sigma)_{\text{max}}$	<0.0001	<0.0001	<0.0001
$\Delta\rho_{\text{max}}$, $\Delta\rho_{\text{min}}$ (e Å ⁻³)	0.27, -0.18	0.31, -0.18	0.36, -0.18
Extinction method	<i>SHELXL</i>	<i>SHELXL</i>	<i>SHELXL</i>
Extinction coefficient	0.074 (12)	0.050 (10)	0.035 (10)

† Computer programs used: *SMART* and *SAINT* (Bruker, 1998), *SHELXS97* (Sheldrick, 1990), *SHELXL97* (Sheldrick, 1997), *SHELXTL* (Bruker, 2000).

and then cooled to the required temperature. The data sets are referred to as 300, 250, 200, 150 and 90 K, hereafter. After the five sets of data collection, another data set was collected at 300 K. The agreement of these data (300 K2) with 300 K and, therefore, the reversibility of the crystal structural change with temperature was confirmed. Then the crystal was flash-cooled to 90 K. The flash cooling was carried out according to the procedure described in the literature (Harada & Ogawa, 2004). Two consecutive measurements were carried out at this temperature (90 K2 and 90 K3). No difference between 90 K2 and 90 K3 was observed. The crystal was warmed to room temperature for annealing, and then cooled slowly to 90 K at the rate 1 K min⁻¹. An X-ray diffraction analysis was carried out at 90 K (90 K4). Afterwards the crystal was warmed to room temperature and the diffraction analysis was carried out at 300 K (300 K3). The results from 300 K3 showed no difference from those of 300 K and 300 K2, which confirmed the total reversibility of the crystal structural change with temperature. Results obtained from 300 K2, 90 K2, 90 K3, 90 K4 and 300 K3 are given in the supplementary material.¹

For nondisordered molecules all the H atoms were located from difference-Fourier electron density maps and refined isotropically, and all C, N and O atoms were refined anisotropically. For disordered molecules the refinement procedures are given in *Appendix A*.

¹ Supplementary data for this paper are available from the IUCr electronic archives (Reference: BK5008). Services for accessing these data are described at the back of the journal.

3. Results and discussion

3.1. Crystal structure of (1)

There are two crystallographically independent molecules (referred to as molecules *A* and *B* hereafter) in the asymmetric unit (monoclinic, $P2_1/n$, with $Z = 8$). Perspective views of the molecules are shown in Fig. 3. For molecule *A* no disorder was observed at any temperature.

For molecule *B*, a disorder similar to that observed in crystals of (*E*)-stilbenes or azobenzenes was detected at room temperature (Fig. 3). The populations of the two orientations refined to 0.900 (3):0.100 (3). The population of the minor orientation decreased as the temperature was lowered. At 200 K the difference Fourier synthesis gave a few weak residual peaks corresponding to the atoms of the minor orientation in the vicinity of the C=N bond. Refinement with the disorder model was not successful, however, because of the small population of the minor orientation. At 90 K no residual peaks corresponding to atoms of the minor orientation could be detected. The temperature dependence of the populations of the two orientations clearly shows that the disorder is dynamic and that a conformational change takes place in the crystal of (1). The conformational change can be explained to take place through the pedal motion resembling that observed in the crystals of (*E*)-stilbenes and azobenzenes.

3.2. Crystal structure of (2)

The crystal structure observed at room temperature is identical with that reported in the literature (monoclinic unit

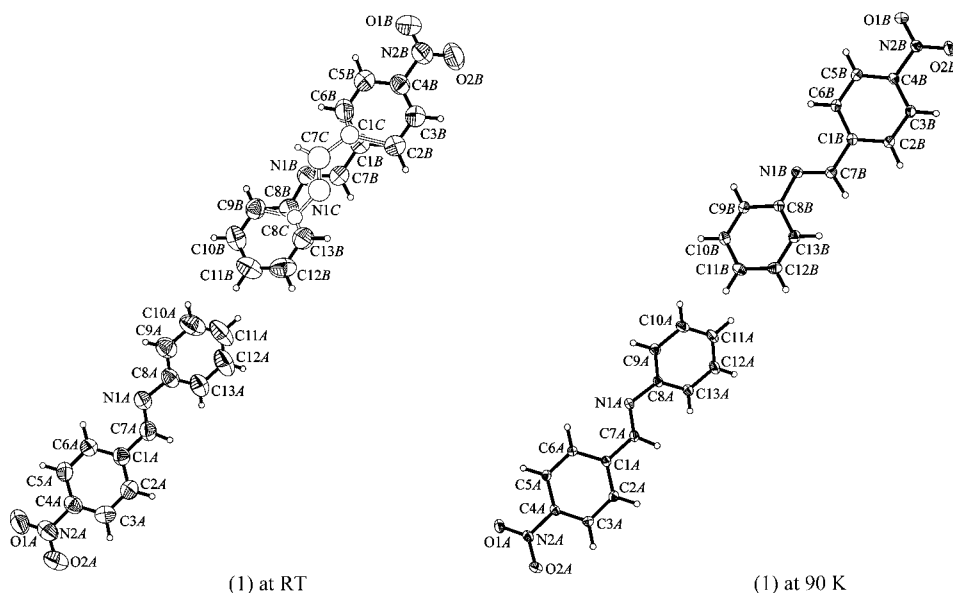


Figure 3 Perspective views of *N*-(4-nitrobenzylidene)aniline (1) with the atom-numbering scheme. The ellipsoids are drawn at the 50% probability level. H atoms are shown as spheres of a fixed arbitrary size. The major molecule at room temperature is drawn with filled bonds and shaded ellipsoids. The minor molecule is drawn with open bonds and spheres.

cell, $P2_1/a$, with $Z = 2$; Bar & Bernstein, 1983; Haller *et al.*, 1995). A perspective view of the molecule is shown in Fig. 4.

The crystal structure of (2) was reported to exhibit a four-fold disorder, as illustrated in Fig. 5. Each molecule in the crystal adopts one of four alternative orientations. Orienta-

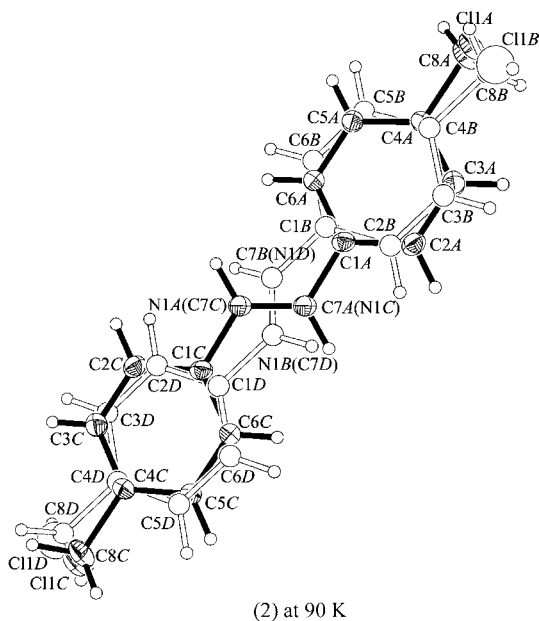


Figure 4 Perspective view of the *N*-(4-chlorobenzylidene)-4-methylaniline (2) with the atom-numbering scheme. The ellipsoids are drawn at the 50% probability level. H atoms are shown as spheres of a fixed arbitrary size. The major molecule is drawn with filled bonds and shaded ellipsoids. The minor molecule is drawn with open bonds and spheres.

tions *A* and *B* are related by a pseudo-twofold rotation around the longest axis of the molecule. The relationship between the two orientations is similar to that in the disordered crystals of (*E*)-stilbenes and azobenzenes. Orientations *A* and *C* are related by inversion. The relationship between orientations *B* and *D*, and that between *C* and *D*, are identical with that between *A* and *C*, and *A* and *B*, respectively. Disorder arising from the coexistence of two or more molecular orientations at the same site is frequently observed in the crystal structures of *N*-benzylideneanilines (Bernstein & Schmidt, 1972; Bernstein & Izak, 1975, 1976; Bar & Bernstein, 1982, 1987). The presence of two molecules ($Z = 2$) in the unit cell of the $P2_1/a$ crystal of (2) requires crystallographic disorder

around an inversion center. Consequently, the population of orientation *A* is equal to that of *C*. The same holds for the relationship between *B* and *D*. However, the populations of orientations *A* and *B* are not necessarily equal.

Refinement with the disorder model gave a ratio of 0.361 (2):0.139 (2) at room temperature, in good agreement with that reported [0.351 (3):0.149 (3)] (Haller *et al.*, 1995). The ratio was determined to be 0.389 (2):0.111 (2) and 0.408 (1):0.092 (1) at 200 and 90 K, respectively. The temperature dependence of the populations clearly shows that the disorder is dynamic and that a conformational change takes place through the pedal motion.

3.3. Crystal structure of (3)

The crystal structure observed at 300 K is identical with that reported in the literature (monoclinic unit cell, $P2_1/c$, with $Z = 2$; Bernstein *et al.*, 1976). A perspective view of the molecule is shown in Fig. 6.

As reported, the crystal structure of (3) shows fourfold disorder identical to that of crystal (2), except that molecule (3) is homo-disubstituted by methyl groups at its *para* positions (Fig. 5). As in the crystal of (2), the molecule resides on an inversion center. The population of orientation *A* equals that of *C* and is not necessarily equal to that of *B*.

Measurements of the diffraction data of the crystal (3) were carried out according to the procedure described in §2. As in the crystals of (1) and (2), lowering of the temperature increases the population of the major orientation (*A*) and decreases that of the minor orientation (*B*); see Table 2. The

Table 2

 Populations of the two orientations in the crystals of *N*-(4-methylbenzylidene)-4-methylaniline (3).

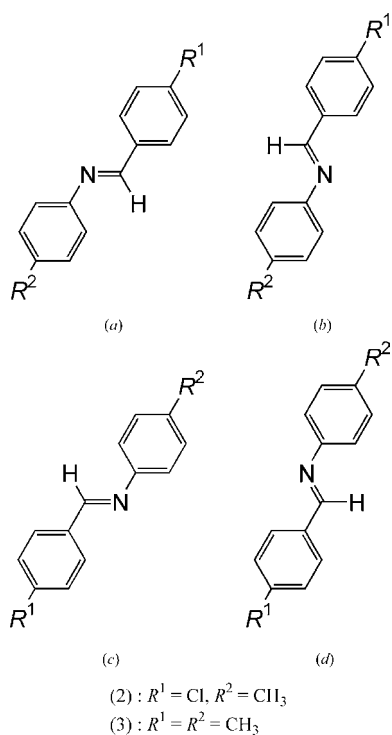
Temperature (K)	
300	0.292 (2):0.208 (2)
250	0.309 (2):0.191 (2)
200	0.333 (2):0.167 (2)
150	0.363 (1):0.137 (1)
90	0.369 (1):0.131 (1)
90 (90 K2†)	0.335 (1):0.165 (1)
90 (90 K4†)	0.369 (1):0.131 (1)

† The definition of the data is given in §2.

temperature dependence of the populations proves that a conformational change also takes place in the crystal of (3).

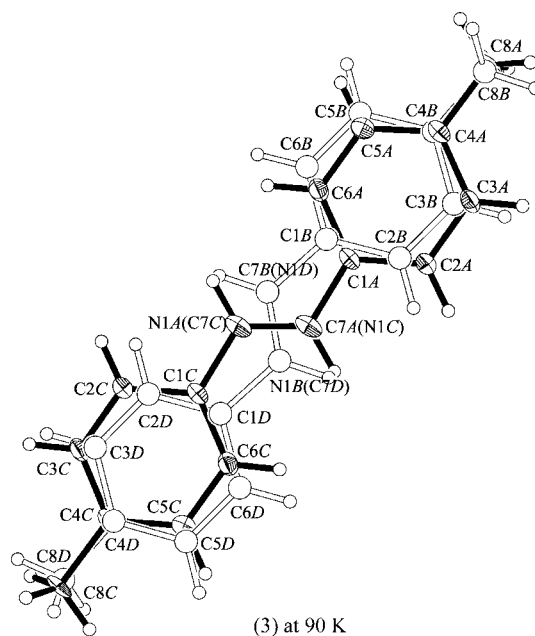
A detailed investigation of the temperature dependence of the populations revealed that the conformational change is frozen in at low temperature. A van't Hoff plot gives an almost straight line in the high-temperature range (300–200 K). At the low-temperature range (200–90 K; Fig. 7), however, the points do not fall on the same straight line.

The populations at 90 K showed a significant dependence on the cooling rate. In the flash-cooled crystal (data 90 K2; see §2), the population of the minor orientation (*B*) increased compared with that in the slowly cooled crystal (90 K and 90 K4).

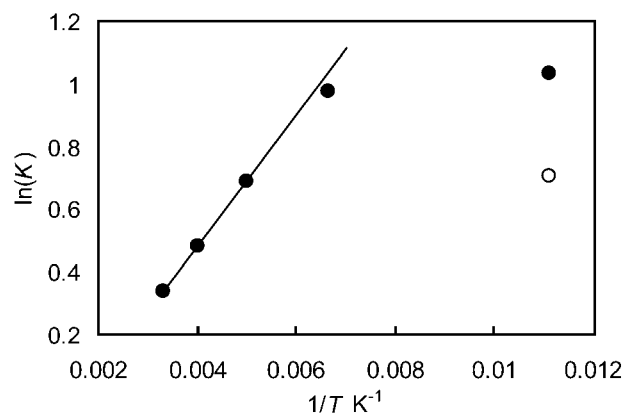

Figure 5

Illustrations of the fourfold disorder in the crystals of *N*-(4-chlorobenzylidene)-4-methylanilines (2) and *N*-(4-methylbenzylidene)-4-methylanilines (3): (a) orientation A, which is the reference orientation; (b) orientation B, which is twofold rotation-related with orientation A; (c) orientation C, which is inversion-related with orientation A; (d) orientation D, which is inversion-related with orientation B.

The nonlinearity of the van't Hoff plot and the cooling-rate dependence of the populations can be explained in terms of a thermodynamic nonequilibrium state generated by a freezing in of the conformational change at low temperature. A similar phenomenon has recently been reported for crystals of (*E*)-stilbene and azobenzene (Harada & Ogawa, 2004). The freezing in of the conformational change during cooling increases the population of the minor orientation compared with the equilibrium state and, accordingly, the van't Hoff plot becomes nonlinear. During the flash cooling, the two orien-


Figure 6

Perspective view of the *N*-(4-methylbenzylidene)-4-methylanilines (3) with the atom-numbering scheme. The ellipsoids are drawn at the 50% probability level. H atoms are shown as spheres of a fixed arbitrary size. The major molecule is drawn with filled bonds and shaded ellipsoids. The minor molecule is drawn with open bonds and spheres.


Figure 7

van't Hoff plot ($\ln K$ versus $1/T$) for the two orientations in the crystal of *N*-(4-methylbenzylidene)-4-methylanilines (3). The data of 300, 250, 200, 150 and 90 K are denoted by filled circles and the data of 90 K2 (flash-cooled) by an open circle. K is the ratio of the populations of the major orientation (orientation A) to that of the minor one (orientation B).

tations in the crystal start to deviate from equilibration at a higher temperature than during the slow cooling, because faster conformational interconversion is necessary for equilibration. Therefore, the deviation from equilibrium and thus the population of the minor orientation is larger in the flash-cooled crystal compared with the crystal which is cooled slowly. The lack of a difference between the two serial data (90 K2 and 90 K3) observed after flash cooling shows that no time evolution of the crystal structure takes place at 90 K during ~ 10 h of data collection time and that the conformational change stops completely at this temperature.

4. Conclusions

In this study we carried out variable-temperature X-ray diffraction analyses of some *N*-benzylideneaniline derivatives: *N*-(4-nitrobenzylidene)aniline (1), *N*-(4-chlorobenzylidene)-4-methylaniline (2) and *N*-(4-methylbenzylidene)-4-methylaniline (3). In the crystal structures of all the compounds a dynamic disorder was observed. The dynamic disorder was accounted for in terms of a conformational change through a pedal motion in the crystals. The results show that the conformational change through the pedal motion is a widespread type of molecular motion in crystals. It was also shown that the conformational change in the crystal of (3) freezes in at low temperature.

APPENDIX A

Refinement of the disordered structures

A1. *N*-(4-Nitrobenzylidene)aniline (1) at room temperature

Only five atoms (N1, C1, C7, C8 and H7) were refined at separate positions in the disorder model (Fig. 3). Four atoms of the major orientation (N1B, C1B, C7B, C8B) were refined anisotropically, and those of the minor orientation (N1C, C1C, C7C, C8C) were refined isotropically. The other non-H atoms were refined anisotropically. The H atoms of the C=N bond (H7B and H7C) were refined according to the riding model. The other H atoms were refined isotropically without any constraint. The length of the C–Ph bond (C1–C7) of the two orientations was restrained to be 1.47 Å with an e.s.d. of 0.01 Å. The length of the N–Ph bond (N1–C8) of the two orientations was restrained to be 1.41 Å with an e.s.d. of 0.01 Å. The length of the C=N bond of the two orientations was restrained to be equal with an e.s.d. of 0.01 Å. Populations were determined from the same refinement as above, except that the eight disordered atoms (N1B, N1C, C1B, C1C, C7B, C7C, C8B and C8C) were refined with a common isotropic temperature factor. The populations were held constant during the subsequent anisotropic refinement.

A2. *N*-(4-Chlorobenzylidene)-4-methylaniline (2)

The overlapping C and N atoms of the orientations *A* and *C* (Fig. 5) were constrained to have the same coordinates, displacement parameters and occupation factors. The same constraints were applied to orientations *B* and *D*. The chlorine

(Cl1) and methyl C (C8) atoms were placed at distances of 1.74 and 1.53 Å from the bonded atom C4 (Fig. 4). They were also fixed on the external bisectors of the angles \angle C3–C4–C5. The benzene rings were constrained to be regular hexagons with bond lengths of 1.39 Å. Non-H atoms of the major orientations (N1A–C1A and N1C–C1C) were refined anisotropically, those of the minor orientations (N1B–C1B and N1D–C1D) were refined isotropically. The chlorine and methyl C atoms of the major orientations were refined with the same anisotropic temperature factors. All N and C atoms of the minor orientations (N1B–C7B and N1D–C7D) were refined with a common isotropic temperature factor. H atoms were refined according to the riding model. Populations were determined from the same refinement as above, except that all atoms were refined isotropically using a common temperature factor for all the N and C atoms and another isotropic temperature factor for the Cl atoms. The populations were held constant during the subsequent anisotropic refinement.

A3. *N*-(4-Methylbenzylidene)-4-methylaniline (3)

The overlapping C and N atoms of orientations *A* and *C* (Fig. 5) were constrained to have the same coordinates, displacement parameters and occupation factors. The same constraints were applied to orientations *B* and *D*. The benzene rings of the minor orientations were constrained to be regular hexagons with bond lengths of 1.39 Å. Non-H atoms of the major orientations (N1A–C8A and N1C–C8C) were refined anisotropically (Fig. 6) and those of the minor orientations (N1B–C8B and N1D–C8D) were refined with a single common isotropic temperature factor. H atoms were refined according to the riding model. Populations were determined from the same refinement as above, except that all non-H atoms were refined isotropically using a common temperature factor. The populations were held constant during the subsequent anisotropic refinement.

This work was supported by the Grant-in-Aid for Scientific Research from the Ministry of Education, Culture, Sports, Science and Technology, Japan, and by Mitsubishi Chemical Corporation Fund.

References

- Bar, I. & Bernstein, J. (1982). *Acta Cryst.* **B38**, 121–125.
- Bar, I. & Bernstein, J. (1983). *Acta Cryst.* **B39**, 266–272.
- Bar, I. & Bernstein, J. (1987). *Tetrahedron*, **43**, 1299–1305.
- Bernstein, J., Bar, I. & Christensen, A. (1976). *Acta Cryst.* **B32**, 1609–1611.
- Bernstein, J. & Izak, I. (1975). *J. Cryst. Mol. Struct.* **5**, 257–266.
- Bernstein, J. & Izak, I. (1976). *J. Chem. Soc. Perkin Trans. 2*, pp. 429–434.
- Bernstein, J. & Schmidt, G. M. J. (1972). *J. Chem. Soc. Perkin Trans. 2*, pp. 951–955.
- Bruker (1998). *SMART* and *SAINT*. Bruker AXS Inc., Madison, Wisconsin, USA.
- Bruker (2000). *SHELXTL*, Version 6.10. Bruker AXS Inc., Madison, Wisconsin, USA.
- Bürgi, H. B. (2002). *Faraday Discuss.* **122**, 41–63.
- Cosier, J. & Glazer, A. M. (1986). *J. Appl. Cryst.* **19**, 105–107.

- Galli, S., Mercandelli, P. & Sironi, A. (1999). *J. Am. Chem. Soc.* **121**, 3767–3772.
- Gavezzotti, A. & Simonetta, M. (1982). *Chem. Rev.* **82**, 1–13.
- Gavezzotti, A. & Simonetta, M. (1987). *Organic Solid State Chemistry. Studies in Organic Chemistry 32*, edited by G. R. Desiraju, ch. 11. Amsterdam: Elsevier.
- Haller, K. J., Rae, A. D., Heerdegen, A. P., Hockless, D. C. R. & Welberry, T. R. (1995). *Acta Cryst.* **B51**, 187–197.
- Harada, J., Harakawa, M. & Ogawa, K. (2004). *Acta Cryst.* **B60**, 578–588.
- Harada, J. & Ogawa, K. (2001). *J. Am. Chem. Soc.* **123**, 10884–10888.
- Harada, J. & Ogawa, K. (2004). *J. Am. Chem. Soc.* **126**, 3539–3544.
- Harada, J., Ogawa, K. & Tomoda, S. (1997). *Acta Cryst.* **B53**, 662–672.
- Harada, J., Uekusa, H. & Ohashi, Y. (1999). *J. Am. Chem. Soc.* **121**, 5809–5810.
- Harris, K. D. M. & Aliev, A. E. (1995). *Chem. Br.* pp. 132–136.
- Ito, Y., Hosomi, H. & Ohba, S. (2000). *Tetrahedron*, **56**, 6833–6844.
- McGeorge, G., Harris, R. K., Batsanov, A. S., Churakov, A. V., Chippendale, A. M., Bullock, J. F. & Gan, Z. (1998). *J. Phys. Chem. A*, **102**, 3505–3513.
- Ohba, S., Hosomi, H. & Ito, Y. (2001). *J. Am. Chem. Soc.* **123**, 6349–6352.
- Saito, K., Okada, M., Akutsu, H., Sato, A. & Sorai, M. (2004). *J. Phys. Chem. B*, **108**, 1314–1320.
- Saito, K., Okada, M., Akutsu, H. & Sorai, M. (2000). *Chem. Phys. Lett.* **318**, 75–78.
- Saito, K., Yamamura, Y., Kikuchi, K. & Ikemoto, I. (1995). *J. Phys. Chem. Solids*, **56**, 849–857.
- Sheldrick, G. M. (1990). *Acta Cryst.* **A46**, 467–473.
- Sheldrick, G. M. (1997). *SHELX97*. University of Göttingen, Germany.
- Sheldrick, G. M. (2002). *SADABS*, Version 2.03 and 2.05. University of Göttingen, Germany.
- Ueda, Y., Nakamura, N. & Chihara, H. (1988). *J. Phys. Soc. Jpn*, **57**, 4063–4064.